

of anisotropically constrained water molecules. In contrast, isotropically mobile water in fluid inclusions gives rise to very sharp peaks lacking spinning sidebands.

The use of two magnetic field strengths for  $^1\text{H}$  MAS-NMR studies provides useful information concerning the sources of the residual line widths. In general, improved spectral resolution is obtained at the higher field, albeit to a lesser extent than predicted from the ratio of the field strengths. The lack of strongly field dependent sideband patterns demonstrates that paramagnetic ions do not significantly affect the spectra of the samples investigated.

Measurement of the isotropic chemical shifts enables one to discriminate different environments of hydrous species, in some cases even within the same mineral. These shifts can be used to estimate the strength of hydrogen bonding, as expressed by the O-H...O distance. The chemical shift does not provide a reliable means of distinguishing OH from  $\text{H}_2\text{O}$  groups, since the hydrogen-bonding strengths of these species may be comparable. Such a distinction is more readily accomplished by comparing relative spinning sideband intensities: the extensive dipolar sideband pattern of isolated structural water molecules differs markedly from the less intense sidebands characteristic of isolated OH groups. However, in minerals that contain OH and  $\text{H}_2\text{O}$  groups in close proximity, strong homonuclear dipolar interactions render spectral discrimination of these species impossible.

Both relative and absolute quantitation of the various hydrous species in minerals can be readily accomplished by using a suitable standard such as pyrophyllite as a  $^1\text{H}$  MAS-NMR intensity reference. In this fashion, water contents in minerals down to levels of about 0.1 wt % have been determined in the present study. Two experimental limitations to such quantitative analyses have

been encountered so far. The first one applies to the relatively broad spectra observed for the clustered hydrogen atoms in hydrogarnets, where it has not proven possible to quantitate water present at levels of ca. 0.2 wt %. Higher spinning speeds, or multiple-pulse methods, should help overcome the difficulties associated with relatively broad MAS-NMR peaks. The second limitation arises from the presence of background signals from the probe and contaminants. To the extent that these problems can be overcome, the inherent sensitivity of high field  $^1\text{H}$  MAS-NMR should enable detection of hydrous species at levels below 0.01 wt%  $\text{H}_2\text{O}$ . These and other improvements will greatly enhance the usefulness of  $^1\text{H}$  MAS-NMR as a unique quantitative tool for the study of trace amounts of hydrous species in geology and materials science.

**Acknowledgment.** The NMR studies were conducted at the Southern California Regional NMR Facility, supported by NSF Grant 84-40137. We are also grateful to Chevron Oil Field Research Corp. for their financial support for a MAS-NMR probe. One of us (G.R.R.) acknowledges support by NSF grants EAR 86-18200 and EAR 83-13098.

**Registry No.**  $\text{AlSi}_4\text{O}_{10}(\text{OH})_2$ , 12269-78-2;  $\text{Mg}_3\text{Si}_4\text{O}_{10}(\text{OH})_2$ , 14807-96-6;  $\text{Ca}_2\text{Mg}_5\text{Si}_8\text{O}_{22}(\text{OH})_2$ , 14567-73-8;  $\text{Al}_2\text{SiO}_4[\text{F}_{0.98}(\text{OH})_{0.02}]_2$ , 1302-59-6;  $\text{Na}(\text{Li},\text{Al})_3\text{Al}_6(\text{BO}_3)\text{Si}_6\text{H}_{18}(\text{OH},\text{F})_4$ , 12197-81-8;  $\text{CaBSiO}_4(\text{OH})$ , 1318-40-7;  $\text{AlOOH}$ , 14457-84-2;  $\text{NaCa}_2\text{Si}_3\text{O}_8(\text{OH})$ , 13816-47-2;  $\text{NaAlSi}_2\text{O}_6\cdot\text{H}_2\text{O}$ , 1318-10-1;  $\text{CaSO}_4\cdot 2\text{H}_2\text{O}$ , 13397-24-5;  $\text{CaB}_3\text{O}_4(\text{OH}_3)\cdot\text{H}_2\text{O}$ , 1318-33-8;  $\text{Zn}_4\text{Si}_2\text{O}_7(\text{OH})_2\cdot\text{H}_2\text{O}$ , 12196-21-3;  $\text{CaAl}_2\text{Si}_2\text{O}_7(\text{OH})_2\cdot\text{H}_2\text{O}$ , 1318-81-6;  $\text{KAlSi}_3\text{O}_8$ , 12251-43-3;  $(\text{NH}_4,\text{K})\text{AlSi}_3\text{O}_8$ , 12418-12-1;  $(\text{Na},\text{K})\text{AlSiO}_4$ , 1302-72-3;  $\text{SiO}_2$ , 14808-60-7;  $\text{Ca}_3\text{Al}_2(\text{SiO}_4)_3$ , 1302-57-4;  $\text{HO}$ , 3352-57-6.

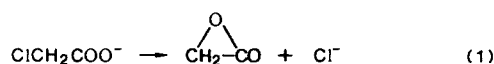
## Theoretical Study of $\alpha$ -Lactone, Acetoxy Diradical, and the Gas-Phase Dissociation of the Chloroacetate Anion

Danko Antolovic, Vernon J. Shiner, and Ernest R. Davidson\*

Contribution from the Department of Chemistry, Indiana University, Bloomington, Indiana 47405. Received December 26, 1986

**Abstract:** The influence of the  $\alpha$ -carboxylate group on the mechanism and energetics of the departure of the chloride anion from chloroacetate was investigated theoretically for a gas-phase reaction. Ab initio Hartree-Fock and configuration-interaction methods were used to obtain the energy values along the reaction path, as well as a description of the intermediate states. Several basis sets were utilized and the results compared. It was found that the three-membered ring of the  $\alpha$ -lactone closes simultaneously with the departure of the electrophile and that a loosely bound complex is formed in the process. Acetoxy zwitterion and diradical were also investigated in detail. The zwitterion is high in energy. The diradical has many states that are similar to the isoelectronic trimethylene methane but with the symmetry instability problems found previously for formyloxyl.

In this paper we report a quantum chemical investigation of the mechanistic and energetic aspects of the gas-phase reaction (1). This reaction is a computationally accessible model, which



we investigate with the aim of shedding additional light on the role of the  $\alpha$ -carboxylate group in nucleophilic substitution reactions. Our primary objective in this work was to determine whether the reaction follows an  $\text{S}_{\text{N}}1$  or an internal  $\text{S}_{\text{N}}2$  mechanism, i.e. whether the departure of the halogen and the closing of the ring constitute two separate events or a single, concerted process.

A second objective was to study in detail the acetoxy diradical, which has many features in common with the isoelectronic trimethylenemethane and formyloxyl radicals. The acetoxy radical

has sometimes been described as a zwitterion so we have also investigated this possibility.

### Nucleophilic Substitutions

The process observed in the laboratory was not the gas-phase reaction (1) but the nucleophilic substitution reaction in solution (eq 2). The main effects of the carboxylate group close to the



substitution site consist of an increase in the reaction rate (relative to similar substitutions without the carboxylate) and the retention of stereochemical configuration at the substitution site.<sup>1</sup> The

(1) Cowdrey, W. A.; Hughes, E. D.; Ingold, C. K. *J. Chem. Soc.* 1937, 1208; 1938, 1243. Grunwald, E.; Winstein, S. *J. Am. Chem. Soc.* 1948, 70, 841.

kinetics of reaction 2 are of the first order in the reactants, indicating a stepwise  $S_N1$  mechanism (eq 2a,b), which would



normally lead to racemization. In order to explain these phenomena, especially the unexpected absence of racemization, the intermediate species of this reaction has been described as an  $\alpha$ -stabilized zwitterion,<sup>2</sup> or an  $\alpha$ -lactone.<sup>3</sup>

In recent work, Shiner and McMullen<sup>4</sup> investigated the solvolyses of the 2-bromophenylacetic and 2-(*p*-tolylsulfonyl)propionic acids in water and ethanol-water solvents. Their results on the deuterium isotope effects are consistent with the formation of an ion-pair zwitterion intermediate, which could be further stabilized by a ring-closing interaction of the substitution site with the  $\alpha$ -carboxylate group. Whether or not the covalent  $\alpha$ -lactone is formed is believed to depend on the ability of the other substituents at the  $\alpha$ -carbon to stabilize the zwitterion and on the properties of the solvent in which the reaction takes place.

We show below that the quantum chemical results point toward an internal  $S_N2$  mechanism for the reaction (1), in agreement with the experimentally known facts. However, we must caution against too literal an interpretation of the theoretical results for a simple model, since they do not account for any of the effects that either the solvent or the additional substituents may have upon the course of the nucleophilic substitution reaction. The experimental results quoted above<sup>4</sup> are indicative of an active role played by the solvent.

### Computational Details

At the semiempirical level, geometry optimizations<sup>5</sup> were done by means of the MNDO technique,<sup>6</sup> in order to obtain portions of the energy surface in the vicinity of the reaction path.

Ab initio Hartree-Fock<sup>7</sup> calculations were performed with several basis sets. As the starting point, we used the 3-21G basis,<sup>8</sup> augmented by Huzinaga's d-type polarization functions<sup>9</sup> on all the atoms except hydrogen. This basis was labeled 3-21+d.

To the above basis were added diffuse s- and p-type functions, using the exponents 0.036, 0.0438, and 0.0845 on hydrogen, carbon, and oxygen, respectively. These diffuse functions were obtained by Clark et al.<sup>10</sup> by minimizing the energies of a number of anions. The exponent on chlorine was obtained as an even-tempered extension of the 3-21G set and has the value of 0.0527. The entire augmented basis set was labeled 3-21+d+sp.

The above two sets were used for Hartree-Fock geometry optimizations.<sup>11</sup> Subsequently, single-point Hartree-Fock and CI calculations were performed in a basis obtained by replacing the 3-21G set with the 9s5p split-valence basis, introduced by Dunning and Hay<sup>12</sup> (labeled D95 for brevity), while retaining the polarization and diffuse function described above. This basis was labeled D95+d+sp.

All of the configuration-interaction calculations involved single and double excitations selected by perturbation theory, with the Hartree-Fock configuration as reference. A two-pass INO scheme<sup>13</sup> was used, the first CI calculation using Hartree-Fock K-orbitals<sup>14</sup> and the second using the

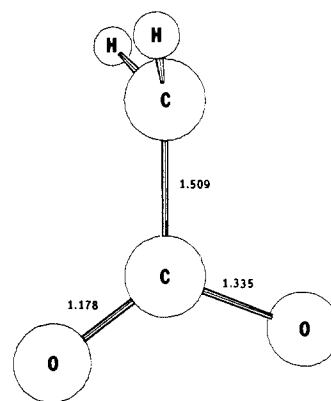


Figure 1. Staggered  $^3A'$  ( $\sigma$ ) state of the acetoxy diradical.

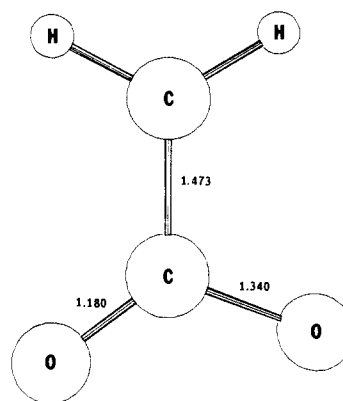


Figure 2. Planar  $^3A''$  ( $\sigma$ ) state of the acetoxy diradical.

natural orbitals obtained from the first. This was done in order to improve the quality of the molecular orbitals. All energy values were extrapolated to the full CI limit by means of a variant of the configuration-interaction extrapolation formula.<sup>15</sup>

Ab initio geometry optimizations were performed by means of the program package GAMESS,<sup>16</sup> and subsequent single-point Hartree-Fock and CI calculations were done with the program MELD.<sup>17</sup> All ab initio computations were done on an FPS 164 array processor, while the MNDO program package, MOPAC,<sup>18</sup> was used on a VAX 11/780.

### Ab Initio Description of Acetoxy

Departure of the chloride anion from the chloroacetate molecule could occur independently of the closing of the lactone ring ( $S_N1$  mechanism) or simultaneously (internal  $S_N2$  mechanism). In the first case, an intermediate, neutral ring-free species would be produced,  $\text{CH}_2\text{COO}$  (acetoxy), which could either undergo rearrangement to acetolactone, or acquire a nucleophile in the subsequent step, without passing through the lactone stage.

An earlier semiempirical study<sup>19</sup> (MINDO/3) of the acetoxy and difluoroacetoxy predicted the existence of both  $\alpha$ -lactones and planar, ring-free zwitterions. The latter are characterized by a closed-shell  $^1A'$  wave function in the Hartree-Fock approximation, and their name is indicative of the alternating atomic charges, which the Mulliken and Löwdin population analyses tend to attribute to such species. The MINDO/3 calculations also described stable peroxide-like molecules, not considered in previous mechanistic hypotheses. Lactones were

(2) Kemp, K. C.; Metzger, D. *J. Org. Chem.* **1968**, *33*, 4165.

(3) Bordwell, F. G.; Knipe, A. C. *J. Org. Chem.* **1970**, *35*, 2956.

(4) McMullen, D. F. (with Shiner, V. J.) Doctoral Dissertation, Indiana University, 1982.

(5) (a) Fletcher, R.; Powell, M. J. D. *Comput. J.* **1963**, *6*, 163. (b) Davidson, W. C. *Comput. J.* **1968**, *10*, 406. (c) Komornicki, A.; McIver, J. W. *Chem. Phys. Lett.* **1971**, *10*, 303.

(6) Dewar, M. J. S.; Thiel, W. *J. Am. Chem. Soc.* **1977**, *99*, 4899.

(7) Roothaan, C. C. J. *Rev. Mod. Phys.* **1951**, *23*, 69.

(8) (a) Binkley, J. S.; Pople, J. A.; Hehre, W. J. *J. Am. Chem. Soc.* **1980**, *102*, 939. (b) Gordon, M. S.; Binkley, J. S.; Pople, J. A.; Pietro, W. J.; Hehre, W. J. *J. Am. Chem. Soc.* **1982**, *104*, 2797.

(9) Huzinaga, S., Ed. *Gaussian Basis Sets for Molecular Calculations*; Elsevier: Amsterdam, 1984; p 24.

(10) Clark, T.; Chandrasekhar, J.; Spitznagel, G. W.; Schleyer, P. v. R. *J. Comput. Chem.* **1983**, *4*, 294.

(11) Schlegel, H. B. *J. Comput. Chem.* **1982**, *3*, 214.

(12) Dunning, T. H.; Hay, P. J. In *Modern Theoretical Chemistry*; Schaefer, H. F., III, Ed.; Plenum: New York, 1976; Vol. 3.

(13) Bender, C. F.; Davidson, E. R. *J. Phys. Chem.* **1966**, *70*, 2675.

(14) Feller, D.; Davidson, E. R. *J. Chem. Phys.* **1981**, *74*, 3877.

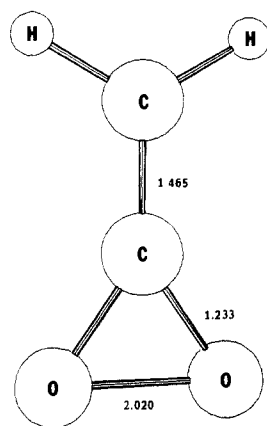
(15) Davidson, E. R. In *The World of Quantum Chemistry*; Daudel, R., Pullman, B., Eds.; Reidel: Dordrecht, 1974.

(16) GAMESS was developed by M. Dupuis, D. Spangler, and J. J. Wendoloski at NRCC and has been subsequently modified by M. Schmidt, and S. Elbert for the FPS 164.

(17) MELD was originally written by L. McMurchie, S. Elbert, S. Langhoff, and E. R. Davidson and has subsequently been modified by D. Feller, and D. Rawlings.

(18) MOPAC was developed by J. J. P. Stewart at the Frank J. Seiler Research Laboratory of the U.S. Air Force Academy.

(19) Chung, C. S. C. *J. Mol. Struct.* **1976**, *30*, 189.

Figure 3. Peroxide form of  $\text{CH}_2\text{COO}$ .

found to be the species of lowest energy.

MNDO calculations by McMullen<sup>4</sup> describe a stable  $\alpha$ -proprionolactone. The corresponding open structure (zwitterion) was found to be unstable, and geometry optimization led to the dissociation of the  $\text{C}_2\text{H}_4\text{-COO}$  bond.

Hartree-Fock geometry optimizations, in the 3-21+d basis, were performed on acetoxyl. These calculations revealed two basic geometries, eclipsed (planar) and staggered, each having several electronic states. The two carbons and two oxygen atoms were found to be coplanar in all cases, and the methylene group was either coplanar with the rest of the molecule or perpendicular to the  $\text{CCOO}$  plane (see Figures 1 and 2).

Of the closed-shell configurations, ring-free zwitterions were found to be of no physical significance; in the planar case, with  $C_s$  symmetry imposed throughout the geometry optimization, no closed-shell minimum was found and the molecule disintegrated to  $\text{CH}_2$  and  $\text{CO}_2$  instead. For the staggered initial geometry, on the other hand, optimization closed the ring without any barrier and yielded the acetolactone molecule. It is interesting to notice that, in the smaller 3-21 basis, one finds a stable, staggered zwitterion structure, some 41.4 kcal/mol above the staggered  $^3A'$ , which is the lowest staggered Hartree-Fock state of  $C_2$  symmetry. The existence of this spurious state must be attributed to the lack of the d-orbitals, which are necessary for an accurate description of the three-membered lactone ring.

Energies of the hypothetical zwitterions, at fixed geometries, provide further argument against the existence of such states. In the planar case, a closed-shell state, at the geometry of the stable  $^3A''$  state, yields a Hartree-Fock energy in the 3-21+d basis, which is 73 kcal/mol above the triplet state. Similarly, a staggered closed-shell state, at the geometry of  $^3A'$ , has an energy 63 kcal/mol above the triplet. These conclusions regarding the high energy of the zwitterion compared to diradicals are in agreement with the recent work of Kahn et al.,<sup>20</sup> which appeared after this paper was submitted. Kahn et al. found that zwitterions are unfavorable compared to diradicals, described by a UHF wave function, for a large number of 1,3-dipoles.

An initial guess to the geometry with the  $\text{O-C-O}$  angle of  $68^\circ$ , rather than  $120^\circ$ , converged to a closed-shell, planar peroxide structure, close to that described by MINDO/3 (see Table I and Figure 3). This species differs from the intermediates described below, having a  $\sigma$  skeleton in the  $\text{COO}$  ring and a bonding,  $\pi$ -( $\text{C-C}$ ) HOMO.

A formal analogy can be drawn between the rearrangement acetolactone  $\rightarrow$  acetoxyl  $\rightarrow$  ethylene peroxide on one hand and the isoelectronic rearrangements of methylenecyclopropane on the other.<sup>21</sup> However, the Hartree-Fock energy of the peroxide, in the 3-21+d basis, is 73.4 kcal/mol higher than that of the lactone, probably because of the presence of an  $\text{O-O}$  bond. Therefore,

Table I. Bond Lengths ( $\text{\AA}$ ), Bond Angles (deg), and Energies (au) of the  $\text{CH}_2\text{COO}$  Species, Optimized in the 3-21G+d Basis<sup>a</sup>

Staggered Conformations ( $C_2$ )					
parameter	$^3A'$ ( $\sigma$ )	$^3A''$ ( $\pi$ )	$^1A'$ ( $\sigma$ )	$^1A''$ ( $\pi$ )	
C—C	1.509	1.492	1.508	1.500	
H—C	1.080	1.078	1.080	1.081	
$\text{C}_2=\text{O}_{\text{cis}}$ <sup>b</sup>	1.178	1.173	1.178	1.174	
$\text{C}_2=\text{O}_{\text{trans}}$	1.335	1.388	1.339	1.384	
H—C—H	117.4	119.4	117.2	117.6	
$\text{HC}_1\text{H}-\text{C}_2$	150.2	172.8	148.9	155.8	
$\text{C}_1-\text{C}_2=\text{O}_{\text{cis}}$	125.5	125.8	125.2	125.0	
$\text{C}_1-\text{C}_2-\text{O}_{\text{trans}}$	112.3	114.0	113.3	114.7	
energy	-225.4447	-225.4255	-225.4424	-225.4241	
Staggered Conformations ( $C_{2v}$ , Constrained)					
parameter	$^3A_1$ ( $\sigma$ )	$^3B_1$ ( $\pi$ )	$^3A_2$ ( $\pi$ )		
C—C	1.486	1.495	1.469		
H—C	1.077	1.078	1.082		
C—O	1.233	1.244	1.290		
H—C—C	119.8	120.2	120.2		
C—C—O	125.6	120.4	117.5		
O—C—O	108.8	119.2	124.9		
energy	-225.4014	-225.3995	-225.2249		
Planar Conformations ( $C_2$ )					
parameter	$^3A'$ ( $\pi$ )	$^3A''$ ( $\sigma$ )	$^1A'$ ( $\pi$ )	$^1A''$ ( $\sigma$ )	
C—C	1.458	1.473	1.473	1.472	
$\text{H}_{\text{cis}}-\text{C}^c$	1.077	1.077	1.077	1.077	
$\text{H}_{\text{trans}}-\text{C}$	1.076	1.078	1.077	1.077	
$\text{C}_2=\text{O}_1$	1.183	1.180	1.174	1.179	
$\text{C}_2=\text{O}_2$	1.378	1.340	1.399	1.347	
$\text{H}_{\text{cis}}-\text{C}_1-\text{C}_2$	119.0	117.6	119.0	117.6	
$\text{H}_{\text{trans}}-\text{C}_1-\text{C}_2$	120.3	121.6	120.0	121.6	
$\text{C}_1-\text{C}_2=\text{O}_1$	124.9	126.6	125.7	126.5	
$\text{C}_1-\text{C}_2=\text{O}_2$	114.5	111.3	113.5	112.1	
energy	-225.4399	-225.4573	-225.4344	-225.4548	
Planar Conformations ( $C_{2v}$ , Constrained)					
parameter	$^3A_2$ ( $\sigma$ )	$^3B_2$ ( $\pi$ )	$^3A_1$ ( $\pi$ )	$^1A_2$ ( $\sigma$ )	peroxide
C—C	1.459	1.379	1.479	1.465	1.301
H—C	1.078	1.078	1.077	1.077	1.078
C—O	1.234	1.283	1.299	1.233	1.320
H—C—C	119.4	120.2	119.2	119.3	120.0
C—C—O	125.0	120.6	117.7	125.0	145.9
O—C—O	110.0	118.8	124.6	110.0	68.1
energy	-225.4155	-225.4286	-225.2298	-225.4131	-225.3678

<sup>a</sup> $^3B_2$  ( $\sigma$ ), unstable;  $^3B_1$  ( $\sigma$ ), unstable. <sup>b</sup>Oxygen atoms are labeled cis and trans with respect to the tilt of the  $\text{CH}_2$  group. <sup>c</sup>Hydrogen atoms are labeled cis and trans with respect to the doubly bonded oxygen,  $\text{O}_1$ .

we do not expect significant similarity between the potential energy surfaces of these two rearrangements.

The open-shell configurations of the molecule  $\text{CH}_2\text{COO}$  (acetoxyl diradical) should be expected to bear some resemblance to the formylxyl radical,  $\text{HCO}_2^*$ , a molecule exhibiting an SCF instability in the description of the unpaired electron, delocalized over the  $\text{COO}$  group. Specifically, the  $C_{2v}$ -constrained SCF calculations on the formylxyl radical produce wave functions of high energy, which, upon relaxation of the symmetry constraint, collapse discontinuously into wave functions of  $C_s$  symmetry, even if the  $C_{2v}$  geometry is retained. Unconstrained geometry optimizations, at the SCF level, yield strongly asymmetrical geometries of the  $\text{COO}$  group, with the unpaired electron localized on one of the oxygen atoms. Such discontinuous breaking of symmetry does not represent physical reality.

The formylxyl radical was studied by Feller et al.,<sup>22</sup> who found the energy minimum to have a symmetrical geometry, at the CI level of calculation. In a later study, McLean et al.<sup>23</sup> performed large MCSCF calculations on this molecule, confirming the  $C_{2v}$  symmetry of the ground state. By including oxygen orbitals of the 3p type into the active space of the MCSCF calculation (orbital doubling), the latter authors have obtained a symmetrical  $\sigma$  radical.

Within the planar and staggered  $C_s$  conformations of acetoxyl, we performed geometry-optimized SCF calculations on the

(20) Kahn, S. D.; Hehre, W. J.; Pople, J. A. *J. Am. Chem. Soc.* **1987**, *109*, 1871.

(21) Feller, D.; Tanaka, K.; Davidson, E. R.; Borden, W. T. *J. Am. Chem. Soc.* **1982**, *104*, 967.

(22) Feller, D.; Huyser, E.; Borden, W. T.; Davidson, E. R. *J. Am. Chem. Soc.* **1983**, *105*, 1459.

(23) McLean, A. D.; Lengsfeld, B. H., III; Pacansky, J.; Ellinger, Y. *J. Chem. Phys.* **1985**, *83*, 3567.

open-shell singlet and triplet states of both symmetries,  $A'$  and  $A''$ . This amounts to a total of eight forms of acetoxyl, although some of them do not represent true minima on the SCF energy surface, as we shall see below. Their geometries and Hartree-Fock energies, in the 3-21+d basis, are summarized in Table I. Labels  $\sigma$  and  $\pi$  in Table I indicate the character of the COO unpaired electron, which is analogous to the unpaired electron in the formyloxyl radical.

In analogy with the results for the formyloxyl radical,<sup>22</sup> all of the staggered open-shell SCF states have  $C_s$  symmetry, with nonequivalent oxygen atoms. The unpaired electrons are localized on one oxygen atom and the methylene carbon, respectively, and the substantial difference in C-O bond lengths indicates that the  $\pi$ -bonding pair of the carboxyl group is also localized.

The state  $^1A'$  is, of course, very similar to its corresponding triplet,  $^3A'$ , both in geometry and in the electronic structure. We have discovered, however, that the  $^1A'$  state is an artifact of the Hartree-Fock method. When the two unpaired  $a'$  electrons are placed into nonorthogonal spatial orbitals (GVB formalism), geometry optimization yields acetolactone.

Similarly, the state  $^1A''$  is not a minimum on the SCF energy surface. Relaxation of the  $C_s$  symmetry constraint results in a downward slide in energy, toward the state  $^1A'$ . The remaining three staggered states are stable under small perturbations of the  $C_s$  symmetry.

Similar considerations are valid for the planar states. Again, the MO's of the unpaired electrons have p character, the one on the carbon atom being  $a''$ , perpendicular to the  $CH_2$  group. Features of the carboxyl group are the same as in the staggered states. The state  $^1A'$  is a symmetry-constrained stationary point, which turns into  $^1A''$  as soon as the  $C_s$  constraint is relaxed. The other three planar states are true minima on the Hartree-Fock energy surface. Unlike the staggered  $^1A'$  open-shell state, the planar  $^1A''$  also corresponds to a true minimum on the GVB potential surface: unconstrained geometry optimization yields a shallow minimum of planar geometry, but not the acetolactone.

We see that the Hartree-Fock calculations on the asymmetric states, in both conformations, favor the states in which the unpaired COO electron resides in an  $a'$  orbital, in the plane of the carboxylate group ( $\sigma$  radical). This result is similar to that of an MNDO calculation on  $HCO_2^*$ , performed by Dewar et al.,<sup>24</sup> which also incorrectly predicts an asymmetrical  $\sigma$  ground state. Also, the SCF and GVB geometry optimizations have produced only one viable energy minimum on the open-shell singlet surface, the planar  $^1A''$  ( $\sigma$ ) state.

Hartree-Fock geometry optimizations of the lowest triplet states, of both planar and staggered conformations, constrained to the  $C_{2v}$  symmetry, were performed in the 3-24+d basis (see Table I). As expected, they yielded states of higher energy, two of which were found to be dissociative (staggered  $^3B_2$  ( $\sigma$ ) and planar  $^3B_1$  ( $\sigma$ )), breaking up into  $CH_2$  and  $CO_2$ . Subsequently, single-point SCF and CI calculations were done on the  $C_s$  states, as well as on the low-lying  $C_{2v}$  states, in the D95+d+sp basis (see Table II). The geometries used were optimized in the 3-21+d basis. The CI energies were extrapolated to account for configurations not included in the CI.

In general, the planar states of the acetoxyl diradical are not simple variants of the formyloxyl case. These states can be regarded as related to the peroxide form, obtained by the removal of electrons from the  $\sigma^*(O-O)$  orbital, since the C-C bond in the  $^3A_2$  ( $\sigma$ ) and  $^3B_2$  ( $\pi$ ) is shorter than in the corresponding staggered  $^3A_1$  ( $\sigma$ ) and  $^3B_1$  ( $\pi$ ) states (see Table I). The geometry of the  $^3B_2$  ( $\pi$ ) in fact approximates more closely the  $^3A_2$  state of the isoelectronic  $CO_3$  and  $C(CH_2)_3$  diradicals: hence the rather short C-C bond in the  $^3B_2$  ( $\pi$ ) state and a smaller symmetry instability.

As in the case of the formyloxyl radical, configuration-interaction calculations essentially remove the instability observed in the SCF wave function, indicating that both  $\sigma$  and  $\pi$  ground states have  $C_{2v}$  symmetry. However, the energy differences between the

**Table II.** CI Energies (au) of the  $CH_2COO$  Species, in the D95+d+sp Basis

	$E_{HF}$	confign	$E_{extrap}$
Staggered Conformations			
$^3A'$ ( $\sigma$ )	-226.5778	27 264	-227.162
		59 688	-227.159
$^3A''$ ( $\pi$ )	-226.5565	27 701	-227.148
$^3A_1$ ( $\sigma$ )	-226.5346	27 598	-227.158
		56 908	-227.157
$^3B_1$ ( $\pi$ )	-226.5304	29 083	-227.148
Planar Conformations			
$^3A'$ ( $\pi$ )	-226.5702	28 066	-227.164
$^3A''$ ( $\sigma$ )	-226.5894	27 948	-227.176
		60 774	-227.172
$^3A_2$ ( $\sigma$ )	-226.5483	27 795	-227.174
		57 434	-227.173
$^3B_2$ ( $\pi$ )	-226.5579	30 329	-227.171
$^1A''$ ( $\sigma$ )	-226.5869	16 154	-227.173
		35 014	-227.170
$^1A_2$ ( $\sigma$ )	-226.5460	15 974	-227.173
		33 029	-227.170

$C_s$  and  $C_{2v}$  geometries are within the margin of error of these CI calculations. As expected, the SCF instability in the  $\sigma$  state is more difficult to correct. In fact, the staggered  $\sigma$  state,  $^3A_1$ , retains an instability of 1 kcal/mol, relative to  $^3A'$ , within the best results obtained here. This  $^3A_1$  ( $\sigma$ ) state bears a close formal resemblance to the troublesome  $\sigma$  formyloxyl radical.

Earlier work on the planar states of the acetoxyl diradical<sup>25</sup> involving Hartree-Fock geometry optimizations in the 3-21 basis, described the lowest energy planar state as a  $^3A''$  state of  $C_s$  symmetry. Configuration-interaction calculations, in the D95+d+sp basis, yield the planar  $\sigma$  radical, in the  $^3A_2$  state of  $C_{2v}$  symmetry, as the ground state of the acetoxyl diradical molecule. However, this is still 43.3 kcal/mol above the saddle point of the internal  $S_N2$  pathway, described below (see Table III). This rules out  $S_N1$  as the mechanism of the gas-phase reaction (1).

#### Semiempirical (MNDO) Description of the Internal $S_N2$ Reaction Path

A preliminary search of the potential energy surface was made with use of MNDO. At the saddle point, the Cl-C-C angle has a value of  $112^\circ$ , which indicates that the reaction represents a blend of two distinct processes. The first process is an internal  $S_N2$  ring-closing substitution, with chlorine leaving in a direction roughly compatible with the usual  $S_N2$  trigonal-bipyramidal transition-state geometry at the carbon atom. This is followed closely by a complexation, presumably forming hydrogen bonds, which places chlorine in the plane of the (inverted)  $CH_2$  group.

Full geometry optimizations were performed for the chloroacetate, acetolactone, saddle point, and the ionic complex, confirming the latter as a genuine minimum on the potential energy surface. Geometry optimizations, at the semiempirical as well as at the ab initio level, involved no symmetry constraints. In every case, the final symmetry was found to be  $C_s$ , within the accuracy of the optimization, even if no symmetry was imposed and the initial geometries were somewhat distorted. Energy values, obtained at different theoretical levels, are summarized in Table III.

The semiempirical vibrational analysis of the saddle point structure reveals one (and only one) mode with a negative force constant and an imaginary frequency of  $751.9\text{ cm}^{-1}$ . This normal mode involves stretching of the Cl-C bond, as well as closing of the three-atom ring, and represents the reaction coordinate at the saddle point (see Figure 4). The two lowest real modes have frequencies of  $147.0$  and  $224.3\text{ cm}^{-1}$  and represent in-plane ( $a'$ ), and out-of-plane ( $a''$ ) oscillations of the chlorine atom. The frequency of the  $a'$  oscillation is lower than that of the  $a''$ , since the  $a'$  mode corresponds to the outward swinging of the chlorine atom, which accompanies the formation of the ionic complex.

(24) Dewar, M. J. S.; Parker, A. H.; Pierini, A. B. *J. Am. Chem. Soc.* **1982**, *104*, 3242.

(25) Feller, D., private communication.

(26) Hotop, H.; Lineberger, W. C. *J. Phys. Chem. Ref. Data* **1975**, *4*, 539.

Table III. Energy Values along the Internal  $S_N2$  Reaction Path<sup>a,b</sup>

method	chloroacetate	saddle point	ionic complex	lactone + Cl <sup>-</sup>	lactone	chloride
MNDO, opt.	-47.2182 (0.0)	-47.1532 (41.0)	-47.1766 (26.1)	-47.1606 (36.1)	-34.0503	-13.1103
HF, opt. (3-21G+d)	-682.9251 (0.0)	-682.9025 (14.2)	-682.9207 (2.8)	-682.8965 (18.0)	-225.4848	-457.4117
HF, opt. (3-21G+d+sp)	-683.0176 (0.0)	-682.9801 (23.5)	-682.9893 (17.8)	-682.9619 (35.0)	-225.5227	-457.4392
HF (D95+d+sp)	-686.1957 (0.0)	-686.1569 (24.3)	-686.1685 (17.1)	-686.1459 (31.3)	-226.6115	-459.5343
SDCI, extrap (D95+d+sp)	-686.966 (0.0)	-686.931 (22.0)	-686.944 (13.8)	-686.921 (28.2)	-227.232	-459.689

<sup>a</sup>Energies in parentheses are in kilocalories/mole, relative to chloroacetate.

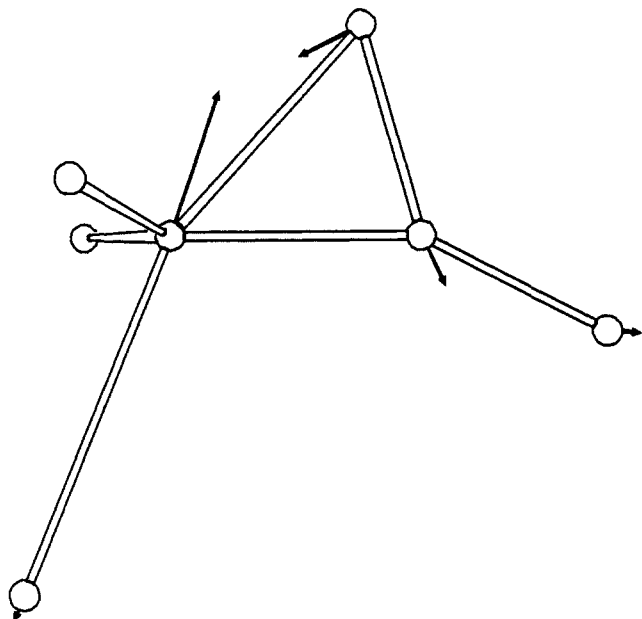


Figure 4. Displacements of nuclei along the reaction path, at saddle point (MNDO).

In the ionic complex, the Cl-C stretching mode has a real frequency of  $91.03\text{ cm}^{-1}$  and the  $a'$  and  $a''$  swinging modes have the frequencies of  $31.50$  and  $50.96\text{ cm}^{-1}$ . As expected, the rest of the vibrational spectrum is very similar to that of the free lactone.

#### Ab Initio Hartree-Fock Description of the Internal $S_N2$ Reaction Mechanism

As mentioned above, Hartree-Fock calculations were performed in the basis sets of increasing size. Geometry optimizations of the four main stages of the reaction were carried out in the 3-21+d and 3-21+d+sp bases. Some preliminary optimizations were done in the pure 3-21 set, leading to the conclusion that the polarization d functions are indeed indispensable for a good description of the three-membered ring of acetolactone.

In order to estimate the need for diffuse s and p functions, we calculated the electron affinity of the  $^2A'$  state of the neutral chloroacetoxy,  $\text{ClCH}_2\text{COO}$ , at the geometry of the chloroacetate anion. At the Hartree-Fock level, the 3-21+d basis yields a value of  $1.98\text{ eV}$  for the electron affinity, and the addition of diffuse functions changes this value to  $3.22\text{ eV}$ . An analogous calculation on the chlorine atom yields an electron affinity of  $2.07\text{ eV}$  in the 3-21+d basis and  $2.61\text{ eV}$  in the 3-21+d+sp basis. By way of comparison, the experimental value of the electron affinity of the chlorine atom is  $3.615\text{ eV}$ .<sup>26</sup>

We see that the addition of diffuse functions reverses the relative magnitudes of electron affinities of the two species, chloroacetate and chlorine, the correction being larger for the former. As seen below (Table III), the dissociation reaction (1) is found to be endothermic. This could be partially attributed to the ring strain in the  $\alpha$ -lactone, but the fact that the charge is being transferred to the species with lower electron affinity certainly corroborates the energetic trend of the reaction. Even though the electron affinities obtained by SCF calculations are not reliable, it is clear that the diffuse basis functions are necessary in order to obtain even a qualitative agreement between the energetics and the relative affinities.

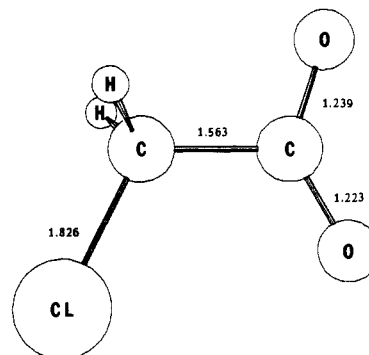


Figure 5. Optimized geometry of chloroacetate (SCF).

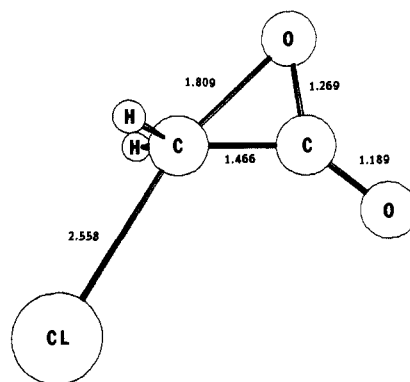


Figure 6. Optimized geometry of the saddle point (SCF).

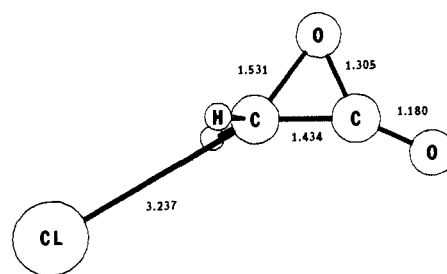


Figure 7. Optimized geometry of the ionic complex (SCF).

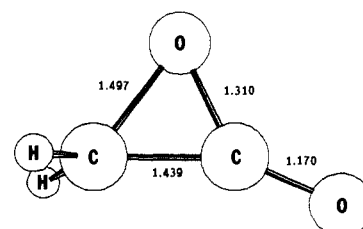


Figure 8. Optimized geometry of acetolactone (SCF).

Geometries obtained in the 3-21+d+sp basis are summarized in Table IV, for the structures shown in Figures 5-8. Corresponding geometries, optimized in the 3-21+d basis, differ insignificantly from the ones obtained in the larger basis. It is worth pointing out that ab initio geometries agree, in a qualitative sense, with the description of the main stages of the reaction obtained by MNDO. In particular, ab initio calculations also confirm the

**Table IV.** Bond Lengths (Å) and Bond Angles (deg) of the Species on the Internal  $S_N2$  Reaction Path (Optimized in the 3-21G+d+sp Basis)

parameter	chloroacetate	saddle point	ionic complex	lactone
C-C	1.563	1.466	1.434	1.439
H-C	1.084	1.071	1.077	1.081
C-Cl	1.826	2.558	3.237	
C <sub>2</sub> -O <sub>cis</sub>	1.223	1.189	1.180	1.170
C <sub>2</sub> -O <sub>trans</sub>	1.239	1.269	1.305	1.310
C <sub>1</sub> -O <sub>trans</sub>	2.295	1.809	1.531	1.497
H-C-H	109.1	119.1	114.9	117.0
HC <sub>1</sub> H-C <sub>2</sub>	125.5	163.9	-168.5	-167.4
Cl-C <sub>1</sub> -C <sub>2</sub>	116.7	122.0	150.2	
C <sub>1</sub> -C <sub>2</sub> -O <sub>cis</sub>	119.2	141.1	154.9	154.9
C <sub>1</sub> -C <sub>2</sub> -O <sub>trans</sub>	109.4	82.5	67.8	65.8

ionic complex as a true minimum on the energy surface.

In order to study the effects of isotopic substitution upon the rate of this reaction, we have performed a vibrational analysis on the Hartree-Fock energy surface, in the 3-21+d basis. Vibrational frequencies of the chloroacetate, the saddle point, and the acetolactone, are listed in Table V, along with the kinetic effects of single and double deuteration.

We find that the reaction rate increases with deuteration, mostly due to the zero-point energy effect. This is in agreement with the calculated values for the force constants, which indicate that the H-C bonds are stronger in the transition state than in the reactant (see also frequencies of the H-C-H symmetric and asymmetric stretch; Table V). However, experimental studies of the isotope effects<sup>4</sup> in similar reactions show a decrease in the rate of reaction. We have no definitive explanation for this discrepancy. It is possible that, under the experimental conditions, the solvent interacts with the hydrogen atoms, weakening the H-C bond in the transition state and thereby reversing the isotopic effect. Also, the actual reaction proceeds on a secondary rather than primary carbon center. This is expected to greatly affect the isotope effect. The fractionation factors at different stages of the ring closure show, on the other hand, that the trend is distinctly different from the change in the -CH<sub>2</sub>- group between propane and cyclopropane (see Table V).

### Configuration Interaction Calculations

A comparison of energy values along the internal  $S_N2$  reaction path, obtained so far by the MNDO and Hartree-Fock methods, reveals substantial methodological discrepancies in the relative energies of the four stages of the reaction, which are of the same magnitude as the relative energies being calculated.

In order to obtain somewhat more believable energy values, we performed single-point calculations of higher quality than those utilized in the geometry optimizations. As the final geometries, we adopted those obtained by optimization in the basis set 3-21+d+sp. Since the basis 3-21 provides a somewhat meager description of the atoms involved, it was replaced with the more complete D95, while the diffuse and polarization functions were retained.

The Hartree-Fock energies in the new basis are also listed in Table III. As can be seen, about 2000 kcal/mol was gained in the total energy, without changing the relative energies by more than 4 kcal/mol, relative to the basis 3-21+d+sp. Further increase in the size of the basis set would be impractical, and unlikely to improve the chemical description substantially, at least at the Hartree-Fock level.

We performed configuration-interaction calculations, the summary of which is given in Table III. Initially, we utilized the SCF orbitals obtained above as the basis for the CI. We used K-orbitals in the virtual space, as the ordinary virtual orbitals tend to be too delocalized to give a good description of the electron correlations. Subsequently, the CI calculation was iterated once, using the natural orbitals of the previous CI calculation as the basis. Orbitals 1s on carbon and oxygen, as well as the orbitals 1s, 2s, and 2p on chlorine, were kept in the core, leaving 48 electrons in the active space. All of the CI calculations were

**Table V.** Frequencies (cm<sup>-1</sup>) of the Normal Modes of Vibration and Corresponding Deuteration Effects (SCF, in the 3-21G+d Basis)<sup>a,b</sup>

	H	1 D	2 D		
Chloroacetate					
C-C rotation	89 (a'')	88	86 (a'')		
	193	192	192		
	407	405	404		
CH <sub>2</sub> , wagging <sup>d</sup>	607 (a'', w)	546 (w)	513 (a'')		
	682	662	643		
	727	714	695		
	914	888 (t)	843 (a'')		
	1024 (a'', t)	931	887		
CH <sub>2</sub> , twisting	1223 (a'')	1021	997 (a'')		
CH <sub>2</sub> , rocking	1339 (r)	1294 (r)	1062		
	1476 (s)	1392 (s)	1162		
CH <sub>2</sub> , sciss	1570	1474	1471		
	1997	1996	1994		
CH <sub>2</sub> , sym str	3243 (Ds)	2399 (ss)	2356		
CH <sub>2</sub> , asym str	3311 (a'', Hs)	3290 (as)	2460 (a'')		
Saddle Point					
reaction	745i	727i	718i		
	188 (a'')	185	181 (a'')		
	262	257	255		
	435	432	428		
	563 (a'', w)	500 (w)	467 (a'')		
	687	677	651		
	974 (t)	817 (t)	757 (a'')		
CH <sub>2</sub> , twisting	999 (a'')	936 (r)	898		
CH <sub>2</sub> , wagging	1109 (a'')	1011	947		
CH <sub>2</sub> , rocking	1233 (r)	1161	955 (a'')		
	1427 (s)	1382 (s)	1193		
CH <sub>2</sub> , sciss	1535	1436	1425		
	2080	2077	2074		
CH <sub>2</sub> , sym str	3400 (Ds)	2550 (ss)	2468		
CH <sub>2</sub> , asym str	3526 (a'', Hs)	3458 (as)	2633 (a'')		
Acetolactone					
	648	610 (r)	606		
	712 (a'')	676 (w)	614 (a'')		
	922	912	906		
	1087 (t)	973 (t)	941 (a'')		
CH <sub>2</sub> , wagging	1162 (a'', o)	1002	973		
CH <sub>2</sub> , twisting	1259 (a'')	1109	978 (a'')		
	1266 (r)	1262	1080		
CH <sub>2</sub> , rocking	1377	1342 (s)	1257		
CH <sub>2</sub> , sciss	1633 (s)	1495	1331		
	2258	2253	2245		
CH <sub>2</sub> , sym str	3343 (Ds)	2498 (ss)	2437		
CH <sub>2</sub> , asym str	3451 (a'', Hs)	3402 (as)	2573 (a'')		
Chloroacetate: Saddle Point					
	$k_{1D}/k_H$	$k_{2D}/k_H$	$k_{1D}/k_H$	$k_{2D}/k_H$	
rotational	0.951	0.908	zero point	1.059	1.104
vibrational	1.014	1.033	total	1.022	1.035
Fractionation Factors <sup>c</sup> (1 D/H)					
chloroacetate	1.28	propane	1.38		
saddle point	1.31	cyclopropane	1.32		
acetolactone	1.49				

<sup>a</sup>The SDCI energy of chloroacetoxyl was -686.831 and of chlorine was -459.577. Tentative descriptions. CH<sub>2</sub> vibrational modes below 1400 cm<sup>-1</sup> are fairly indistinct. <sup>b</sup>Rate constants and fractionation factors are computed using the SCF harmonic frequencies multiplied by 0.9. <sup>c</sup>At 25 °C, for the exchange reaction HC≡CD + RH → HC≡CH + RD.

limited to single and double excitations from a single reference configuration, and the most important configurations were selected by means of perturbation theory. Finally, energy values were extrapolated to the full CI by means of an extrapolation formula. This last step is rather crucial, since the size consistency of the calculation must be maintained, in order to describe the dissociation properly.

The CI wave function in all cases is dominated by the closed-shell Hartree-Fock configuration. The second largest coefficient of space-orbital products never exceeds the value of 0.06. This,

along with the limited improvement achieved by the INO procedure, indicates that the configuration-interaction calculations bring about only an energy correction to a qualitatively adequate Hartree-Fock picture.

Relative energies obtained in the bases 3-21+d+sp and D95+d+sp agree within 3 kcal/mol; we can, therefore, use the latter as an SCF standard. By comparison, MNDO exaggerates the gap between chloroacetate and all the other species. This can be attributed to the absence of d orbitals, which tends to exaggerate the ring strain in all but the chloroacetate molecule. The saddle point is described particularly poorly: its energy was found to be higher than that of the final products, in contradiction with the results obtained by all other methods. We suspect that the pentacoordination of carbon at the saddle point contributes to the difficulties of MNDO in describing this species.

The ab initio SCF calculations in the basis 3-21+d, on the other hand, underestimate the same gap, presumably through a poor description of the chloroacetate. An inspection of the charge distributions shows that the basis 3-21+d, lacking the diffuse functions, attributes larger alternating charges to neighboring atoms, especially to carbon and hydrogen, while diminishing the charges on the oxygens.

The final CI calculations add an overall correlation energy of 480 kcal/mol to the Hartree-Fock energy in the D95+d+sp basis. A comparison of the relative energies shows a lowering of the dissociative steps by 3 kcal/mol relative to the chloroacetate.

In order to gain more information about the energetics of the electron transfer, we performed a modest CI calculation on the  $^2A'$  ground state of the chloroacetoxyl, in the D95+d+sp basis, which yielded 3.66 eV as the electron affinity of this species. Fairly exhaustive single-double CI calculations produced 3.20 eV for the electron affinity of the chlorine atom. The difference between the two electron affinities (0.46 eV) accounts for roughly one-third of the total endothermicity (1.22 eV) of the reaction (1).

### Summary and Conclusions

Our study argues in favor of an  $\alpha$ -lactone intermediate in the nucleophilic substitution reactions of simple  $\alpha$ -substituted carboxylate anions. We find the acetolactone to be a stable molecule, as opposed to the hypothetical zwitterionic intermediates, and lower in energy than either the peroxide or the ring-free open-shell species, all of which were investigated.

Past studies have attributed absence of racemization to the formation of a pyramidal carbonium ion (Cowdrey et al.<sup>1</sup>), stabilized by the carboxylate in a state of broken  $C_3$  spatial symmetry.

We were unable to find any such states: to the contrary, our results on zwitterions indicate that the hypothetical carbonium intermediates do not exist in the gas phase. The only species whose geometries bear some resemblance to this hypothetical intermediate are the staggered open-shell Hartree-Fock states of the acetoxyl diradical. However, the configuration-interaction calculations have established that the breaking of the  $C_{2v}$  symmetry is an artifact of the single-configuration description of their electronic wavefunctions, in quite close analogy with the known results on the formyloxyl radical. We have found no evidence that a spontaneous lowering of the spatial symmetry of an  $S_N1$  intermediate could be invoked to explain the retention of configuration at the substitution site.

Existence of weakly bound ion pairs is commonly invoked as an explanation of the kinetic phenomena observed on the nucleophilic substitution reactions in solutions.<sup>27</sup> Although the solvent certainly influences the formation of such structures, occurrence of an ionic complex within the "gas-phase" is also believed to provide an explanation for the double well invoked by Brauman and co-workers to explain gas-phase reactions.<sup>28</sup> In papers appearing after this manuscript was submitted, Jorgensen and co-workers<sup>29</sup> also found hydrogen-bonded complexes in the  $S_N2$  reactions  $Cl^- + CH_3OH$ ,  $Cl^- + CH_3OOH$ ,  $Cl^- + HCOCl$ , and  $Cl^- + CH_3COCl$ . For the first two of these, the transition state and final product energies are substantially above the starting ions. The last two have energetics similar to what was calculated here with the transition state below the reactant but about 10 kcal/mol above the hydrogen-bonded complex.

**Acknowledgment.** We express our gratitude to Dr. David Feller, who has made available some unpublished data on the acetoxyl diradical. This material is based upon work supported by the National Science Foundation under Grants No. CHE-83-09446, CHE-84-05851, and CHE-85-03415.

**Registry No.**  $ClCH_2CO_2^-$ , 14526-03-5.

(27) (a) Benfrey, O. T.; Hughes, E. D.; Ingold, C. K. *J. Chem. Soc.* **1952**, 2488. (b) Winstein, S.; Clippinger, E.; Fainberg, A. H.; Robinson, G. C. *Chem. Ind. (London)* **1954**, 664. (c) Shiner, V. J., Jr. In *Isotope Effects in Chemical Reactions*; Collins, C. J., Bowman, N. S., Eds.; Van Nostrand Reinhold: New York, 1970. (d) Shiner, V. J., Jr.; Fisher, R. D. *J. Am. Chem. Soc.* **1971**, *93*, 2553.

(28) Olmstead, N. N.; Brauman, J. J. *J. Am. Chem. Soc.* **1977**, *99*, 4219.

(29) (a) Evanseck, J. D.; Blake, J. F.; Jorgensen, W. L. *J. Am. Chem. Soc.* **1987**, *109*, 2349. (b) Blake, J. F.; Jorgensen, W. L. *J. Am. Chem. Soc.* **1987**, *109*, 3856.